

High-Pressure Solidification of Ternary Al-Ni-Sn Alloy

Xiaohong Yang ^{1,2,*}, Feng Lv ^{1,2}, Xiaohong Wang ³ , Zhengzhong Zhang ^{1,2}, Dongdong Zhu ³ , Yuan Chen ^{1,2}, Jianya Ge ^{1,2} and Jinhua Tang ¹

- ¹ Academician Expert Workstation, Jinhua Polytechnic, Jinhua 321017, China; 20191045@jhc.edu.cn (F.L.); 20101023@jhc.edu.cn (Z.Z.); 20191044@jhc.edu.cn (Y.C.); 20050567@jhc.edu.cn (J.G.); JH_tjh@163.com (J.T.)
² Key Laboratory of Crop Harvesting Equipment Technology of Zhejiang Province, Jinhua 321017, China
³ Key Laboratory of Air-Driven Equipment Technology of Zhejiang Province, Quzhou University, Quzhou 324000, China; hitxiaohong_wang@hotmail.com (X.W.); zhudd8@163.com (D.Z.)
* Correspondence: jhyxh656593@163.com; Tel.: +86-180-9126-9296

Abstract: The microstructure, phase composition and mechanical properties of ternary Al-5.4Ni-2Sn (mass fraction) alloy solidified under different high pressures were researched. The results show that the phase composition of the alloy solidified at different pressures is Al, Al₃Ni and β-Sn. The thermodynamic phase diagram of the ternary alloy Al-5.4Ni-2Sn was calculated under the equilibrium condition. The results demonstrate that the solidification process is as follows: L → Al₃Ni → (α-Al + Al₃Ni)_{eutectic} → (α-Al + Al₃Ni + β-Sn)_{eutectic}. The hardness values of α-Al phase at ambient pressure, 2 GPa and 4 GPa are 1.5 GPa, 1.62 GPa and 1.99 GPa, respectively. This is an increase of 8% and 32.7%, respectively. The hardness of β-Sn phase decreases by about 31.2% at 4 GPa. When the deformation is 30%, the compressive strength at ambient pressure, 2 GPa and 4 GPa is 538.1 MPa, 1403.2 MPa and 1547.9 MPa, respectively. The compressive strength under high pressure increased by 160.85% and 187.7%, respectively.

Keywords: high-pressure solidification; Al-Ni-Sn alloy; divorced eutectic; phase composition; compressive mechanical property; nano-hardness



Citation: Yang, X.; Lv, F.; Wang, X.; Zhang, Z.; Zhu, D.; Chen, Y.; Ge, J.; Tang, J. High-Pressure Solidification of Ternary Al-Ni-Sn Alloy. *Crystals* **2022**, *12*, 1025. <https://doi.org/10.3390/cryst12081025>

Academic Editors: Xiang Li and Bolv Xiao

Received: 17 June 2022

Accepted: 21 July 2022

Published: 23 July 2022

Publisher's Note: MDPI stays neutral with regard to jurisdictional claims in published maps and institutional affiliations.



Copyright: © 2022 by the authors. Licensee MDPI, Basel, Switzerland. This article is an open access article distributed under the terms and conditions of the Creative Commons Attribution (CC BY) license (<https://creativecommons.org/licenses/by/4.0/>).

1. Introduction

Aluminum alloy is a light alloys widely used in structural components, which has excellent mechanical and physical properties [1–3]. With the rapid development of the aerospace and military industries, the properties of aluminum alloys need to be further improved to meet further demands. The comprehensive properties of the alloy can be improved by adding alloy elements for cold working and heat treatment. At the same time, different alloy elements can be selected according to different effects and applicability [4]. It is discovered that the addition of iron group elements (such as Mn, Ti, Cr, Ni, etc.) to aluminum alloy can both upgrade the mechanical strength, corrosion resistance and high-temperature resistance of aluminum alloy [5,6]. The action mechanism of these iron group elements in aluminum alloy has the following possibilities [7,8]. The results show that in the process of aluminum alloy ingot casting, the particles containing iron group elements (dispersed phase) are formed, which hinder the dislocation movement in the alloy, Refine the grain and increase the ability of the alloy to bear strain concentration. Meanwhile, iron group elements form a small needle-like phase in the alloy, which plays the role of whisker strengthening. Another aspect is that after aging, the metastable phase is uniformly dispersed in the matrix, playing the role of precipitation strengthening. Among these iron group elements, Ni can significantly enhance the high-temperature properties and mechanical properties of the aluminum alloy. In order to meet the application requirements of the aluminum alloy at higher temperatures, more and more research has been carried out on the addition of Ni to aluminum. When studying the hardness properties of aluminum alloy, it has been found that the intermetallic compound Al₃Ni can be formed in the Al-rich

phase with a small amount of Ni, which is uniformly dispersed in the aluminum alloy matrix and can significantly improve the hardness of the alloy [9,10]. Zhao Yubing et al. [11] found that Al_3Ni formed in the aluminum matrix can reinforce the alloy. At the same time, fine spherical Ni-rich phase particles refine the internal grains of the alloy. Consequently, the strain resistance of the aluminum alloy is strengthened and the elongation is better. Chen Dahui [12] has confirmed that Ni can improve the mechanical properties and casting properties of aluminum alloy. The mechanism is that the Al_3Ni phase has dramatically high strength and hardness, which can play the role of dispersion strengthening, thus improving the mechanical properties. In addition, the eutectic microstructure of $\alpha\text{-Al}$ and Al_3Ni can reduce the formation of hot cracks and increase the fluidity of alloy melt during solidification. As a result, the casting properties of aluminum alloy have been greatly improved. Therefore, Al-Ni alloy has the advantages of high melting point, low density, good oxidation resistance and corrosion resistance. As another important alloy element, Sn has the properties of low surface tension, good electrical and thermal conductivity, excellent ductility and low melting point, etc., and it is usually added to metals and alloys [13–15] to improve the microstructure and mechanical properties of alloys [16–18]. In particular, adding an appropriate amount of Sn to Al-Ni alloy can reduce the melting temperature, which is very important for high-pressure solidification. Due to the size limitations of equipment and metal samples, the service temperature of some high-pressure equipment cannot be very high.

The solid solution formed after solidification has a tremendous influence on the overall properties of the alloy, and the solid solubility and lattice constant are the two most basic parameters to characterize the structural characteristics of the solid solution. High-pressure solidification expands the solution limit of alloy elements in the Al matrix. When the atomic radius of alloy elements is large or small, the phase lattice of the aluminum matrix will expand, resulting in the effect of solid solution strengthening [19–21]. The alloy solidified at higher pressure can not only refine the grain size and modify the phase distribution and composition, but also obtain various non-equilibrium structures. For example, amorphous can be formed under high pressure. It can also improve the distribution and diffusion coefficient of alloy elements, and alter the morphology of the solid–liquid interface [22–24]. When the high pressure (GPa level) is applied to the solidification process of the alloy, the structure of the solid solution formed in the alloy is different from that in the normal pressure solidification due to the effect of changing the atomic spacing and reducing the atomic diffusion system, which affects the properties of the alloy [25–27]. However, the high-pressure solidification technique is rarely used in multicomponent alloys. Therefore, the preparation of Al-Ni-Sn ternary alloy by high-pressure solidification is of great significance to enrich the theoretical research of high-pressure solidification.

Based on the above analysis, the microstructure and the phase composition of the Al-5.4Ni-2Sn alloy prepared at different pressures was observed and analyzed firstly. Then, the thermodynamic phase diagram of Al-5.4Ni-2Sn ternary alloy under equilibrium condition was drawn by panda software. Finally, by testing the mechanical properties of the alloy, the mechanism among the microstructure and properties was established, which provided the corresponding theoretical and experimental data for improving the Al-5.4Ni-2Sn ternary alloy.

2. Experimental Procedures

The nominal composition of the prepared alloy is Al-5.4%Ni-2%Sn, and the raw materials used are pure Al, Ni and Sn (purity 99.99%, Tim (Beijing, China) new material technology Co., Ltd.). Since the melting point of Sn and Al is much lower than that of Ni, Sn and Al have melted before reaching the melting point of Ni, and a small part of Sn has evaporated, especially Sn, which leads to the lower content of Sn and Al in the final solidified Al-5.4Ni-2Sn ternary alloy than the preset content. By adding excessive Sn and Al to compensate for the loss during melting, the Al-5.4Ni-2Sn ternary alloy was prepared by multiple melting and chemical composition detection. The actual chemical composition of

the alloy is analyzed by XRF (zetium XRF, Worcestershire, UK) equipment, and the results are shown in Table 1, which are very close to the nominal composition.

Table 1. Chemical compositions of Al-5.4Ni-2Sn alloy (wt.%).

Al	Ni	Sn
92.63	5.39	1.98

Firstly, Al-5.4Ni-2Sn alloy was melted in an electric arc furnace (DHL-630, Sky Technology Development, Shenyang, China). The alloy composition was considered to ensure that the total weight of each button ingot was no more than 50 g, and the diameter of the melted ingot was about 40 mm. Then, after repeating the melting 5 times, take out the ingot. Use an electric spark wire cutting machine to cut the ingot into cylindrical shape (Φ 6 mm \times 8 mm). Before the high pressure experiment, pyrophyllite, molybdenum sheet, graphite tube, zirconia tube and BN tube were used to assemble the cut sample. After assembly, put it in the middle of six hammers. Then, gradually increase the pressure to the target value (2 GPa and 4 GPa). Maintain the temperature at 1200 °C for 50–60 min. Finally, cool down and depressurize.

The phases were characterized by a Rint 2200 XRD with monochromatic Cu-K α radiation. Morphologies and compositions were investigated on SEM operated at 15 kV equipped with an EDS. The compressive stress–strain curve was measured by a high-temperature testing machine (MTS Landmark 370.10, Rülzheim, Germany). The thermodynamic data of the Al-Ni and Al-Sn systems were collected. The Gibbs free energy model is established according to the thermodynamic function of each phase. Finally, the solidification process of the alloy was calculated based on panda software (Compu. Therm. LLC Co., Ltd., Middleton, WI, USA) and compared with the actual experimental results [28].

3. Results

3.1. Microstructure of Al-5.4Ni-2Sn Alloy Solidified at Different Pressures

The XRD of Al-5.4Ni-2Sn alloy solidified under different pressures is shown in Figure 1. The results indicate that Al phase, Al₃Ni phase and β -Sn phase are the leading phases. Additionally, the pressure did not change the phase composition. From the number of diffraction peaks, it can be observed that the contents of Al phase and Sn phase increase under high pressure. Compared with the results under normal pressure solidification, the diffraction peaks of β -Sn phase appear at 30.74°, 32.12°, 78.26° and 82.5° under 2 GPa, and at 30.8°, 32.2°, 78.36° and 82.6° under 4 GPa, respectively.

The microstructure of Al-5.4Ni-2Sn alloy solidified under different pressures are shown in Figure 2. The results show that the microstructure is composed of a bright phase, gray phase and black phase. Table 2 shows the element contents of the Al-5.4Ni-2Sn alloy after solidification under different pressures. It demonstrates that the content of Sn in the bright white phase is higher, and the mass percentage is 60.07%, 73.91% and 87.62%, respectively. The content of Sn in the black–white phase is only a small part. Meanwhile, when solidified at high pressure, the Ni content in the black phase increases from 0.17% to 0.31%. According to Figure 1, the bright phase is β -Sn, the gray phase is Al₃Ni and the black matrix phase is α -Al. The microstructure of Al-5.4Ni-2Sn alloy solidified at ambient pressure is shown in Figure 2a,b, which shows that the alloy is composed of bulk Al₃Ni phase, bright white β -Sn phase and eutectic phase. Furthermore, the bright white β -Sn phase and the Al₃Ni phases form a sandwich structure. The eutectic microstructure is spherical, which is composed of α -Al phase and Al₃Ni phase. With the increase of solidification pressure, the microstructure of the alloy had barely changed. However, the thickness of the β -Sn phase decreases with the increase of pressure, and the sandwich structure of β -Sn phase and Al₃Ni phase gradually disappears. Instead, the β -Sn phase tends to become enveloped by the Al₃Ni phase.

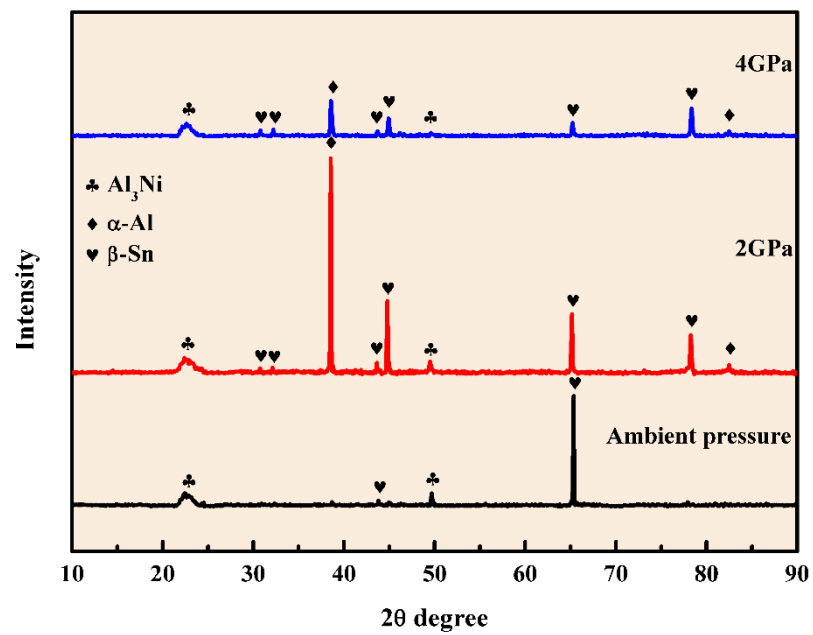


Figure 1. The phase composition of Al-5.4Ni-2Sn alloy solidified under different pressures.

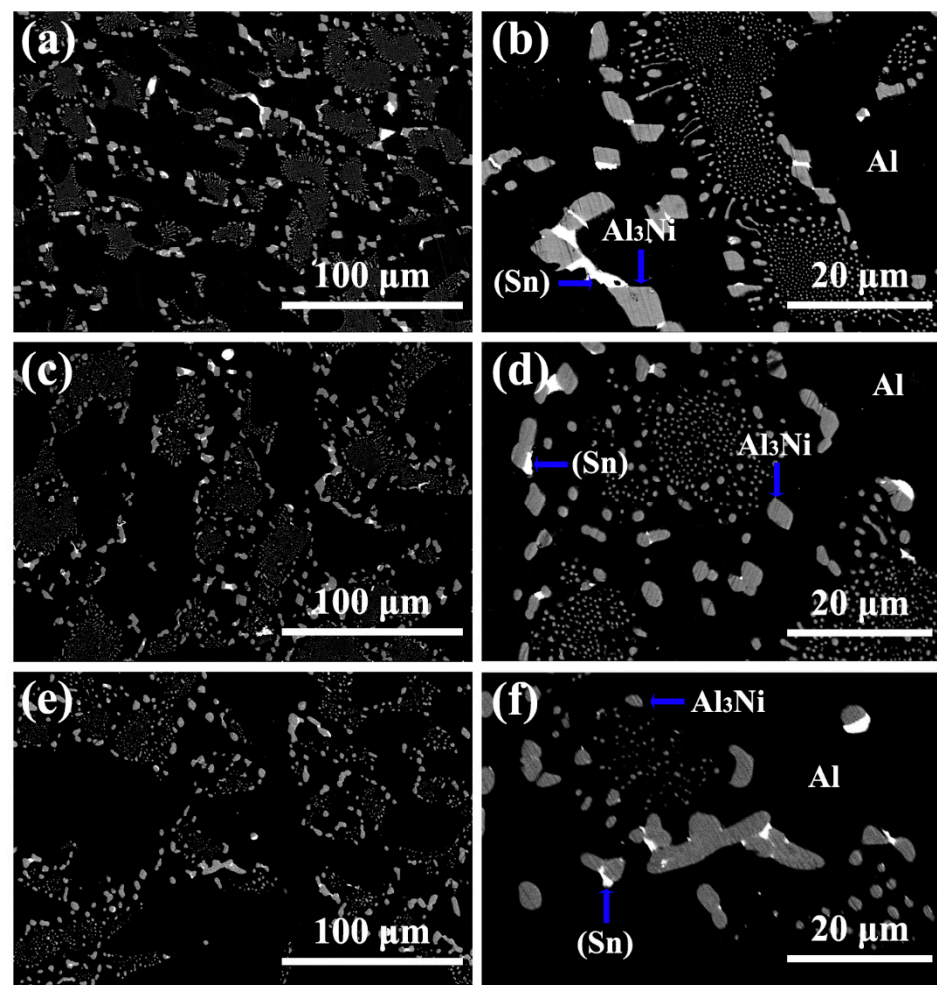
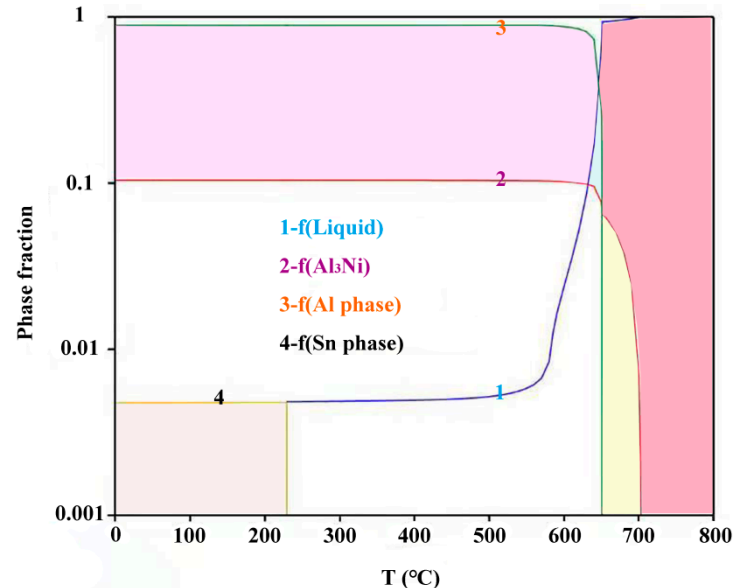


Figure 2. The microstructure of Al-5.4Ni-2Sn alloy solidified under different pressures. (a,b) Ambient pressure, (c,d) 2 GPa, (e,f) 4 GPa.

Table 2. The EDS analysis of the phases under different pressures.

Phase	Atom	Ambient Pressure	2 GPa	4 GPa
Black phase	Ni (wt.%)	0.17	0.25	0.31
	Al (wt.%)	97.59	97.26	96.74
	Sn (wt.%)	2.23	2.49	2.95
White phase	Ni (wt.%)	3.49	3.02	2.7
	Al (wt.%)	36.43	23.07	9.68
	Sn (wt.%)	60.07	73.91	87.62

The phase content of Al-5.4Ni-2Sn alloy at different temperatures during ambient pressure solidification calculated by Pandat software was shown in Figure 3. It can be seen from the figure that the Al₃Ni phase starts to precipitate from the liquid phase when cooling down to 702 °C, and then the content of Al₃Ni phase suddenly changes with the continuous decrease of temperature at 652 °C. At the same time, the content of α-Al phase appears instantaneously in the temperature range of about 20 °C, and then slightly increases with the content of Al₃Ni phase. Soon the content of Al₃Ni phase approaches the maximum, which indicates that eutectic transformation occurs at 652 °C: $l \rightarrow \alpha\text{-Al} + \text{Al}_3\text{Ni}$. Then, in a long solidification temperature range, the content of liquid phase decreased slightly, while the volume fraction of α-Al phase and Al₃Ni phase remained almost unchanged until the ternary eutectic reaction occurred at 229 °C ($l \rightarrow \alpha\text{-Al} + \text{Al}_3\text{Ni} + \beta\text{-Sn}$). Therefore, the sequence of solidification precipitation of Al-5.4Ni-2Sn alloy is $L \rightarrow \text{Al}_3\text{Ni} \rightarrow (\alpha\text{-Al} + \text{Al}_3\text{Ni})_{\text{eutectic}} \rightarrow (\alpha\text{-Al} + \text{Al}_3\text{Ni} + \beta\text{-Sn})_{\text{eutectic}}$. However, the precipitation sequence does not change under high pressure. The solidification pressure of 4 GPa is not enough to change the crystallization process of the alloy.

**Figure 3.** The phase calculation under ambient pressure using the Pandat software.

Based on the analysis, the schematic diagram of the growth of β-Sn phase at different pressures was shown in Figure 4. When the ternary eutectic reaction takes place at 229 °C, as a large number of primary Al₃Ni phases already exist, the Al₃Ni phase generated during the ternary eutectic reaction takes the pre-formed Al₃Ni phase as the nucleation matrix and grows; meanwhile, primary solidified α-Al phase also acts as the substrate for α-Al phase, and eventually divorced eutectic occurs. According to EDS analysis, the content of Sn in β-Sn phase is far more than the initial composition. Therefore, its growth must be in the Sn-rich region. It can be seen from Figure 3 that only the nucleation and growth of Al₃Ni phase can provide the conditions for Sn enrichment. Therefore, the growth of

β -Sn must be carried out in the form of lamellar eutectic with Al_3Ni phase. When Al_3Ni phase is preferentially nucleated and grown from L phase, a large amount of Al and Ni elements are needed, while the excess Sn elements will be discharged and gathered between Al_3Ni phases, which provides conditions for the nucleation of β -Sn phase. When the alloy solidifies under pressure, the pressure has a great inhibition on the diffusion of Ni and Sn elements. Hence, the lamellar growth mode is destroyed, and the β -Sn phase grows surrounded by Al_3Ni phase.

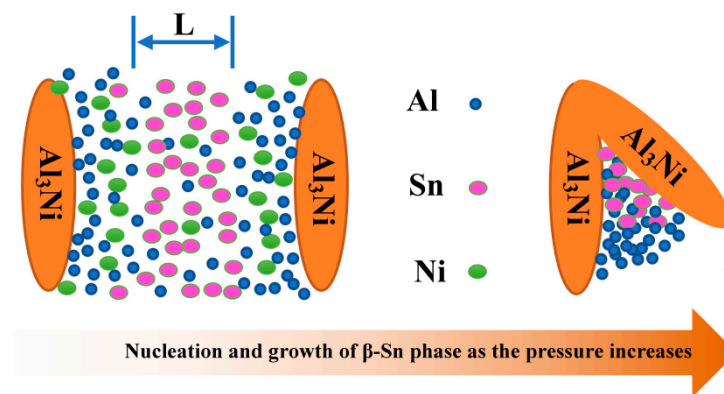


Figure 4. Schematic diagram of the growth of β -Sn phase at different pressures.

3.2. Mechanical Properties of Al-5.4Ni-2Sn Alloy Solidified at Different Pressures

The compressive stress strain curves of Al-5.4Ni-2Sn alloy solidified under different pressures are shown in Figure 5 and the strain rates are 0.001/s. It can be seen that the compressive strength and strain of the Al-5.4Ni-2Sn alloy are obviously improved compared with the samples solidified at ambient pressure. However, there is no obvious yield behavior in the curves, and the curves show the exponential form, reflecting the obviously plastic deformation characteristics. By comparing the trend of mechanical properties in Figure 5, it can be found that Al-5.4Ni-2Sn alloy has the highest compressive strength and higher strain at 4 GPa, while the samples prepared at ambient pressure have the highest strain. When the deformation is 30%, the compressive strength at ambient pressure, 2 GPa and 4 GPa is 538.1 MPa, 1403.2 MPa and 1547.9 MPa, respectively. At the same compressive strength of 500 MPa, the compressive strain at ambient pressure, 2 GPa and 4 GPa are 29.2%, 19.5% and 18.3%, respectively. Under high pressure, the compressive strain decreases by 33.2% and 37.3%, respectively. From the above analysis, it can be seen that under high pressure, the strength value is greatly improved and the plasticity is slightly reduced.

It can be seen from Figures 1 and 2 that the microstructure, phase composition and average size of Al_3Ni phase of Al-5.4Ni-2Sn alloy have no obvious changes under high-pressure solidification conditions. Nevertheless, it can be seen from Figure 5 that the strength of the alloy prepared under high pressure has been greatly improved. Combined with the test results in Table 2, it can be seen that the Ni and Sn content in the α -Al phase is quite different under different pressures. Therefore, it is necessary to consider the solid solution strengthening. The reason for this is that the atoms in the origin array will deviate from the equilibrium position, resulting in lattice distortion, which makes it difficult to carry out dislocation in the alloy and increases the strength of the alloy. Meanwhile, the crystal lattice distortion will be caused when the solute atoms dissolve into the lattice by adding alloy elements, and the scattering effect of the distorted lattice on the moving atoms will be intensified accordingly.

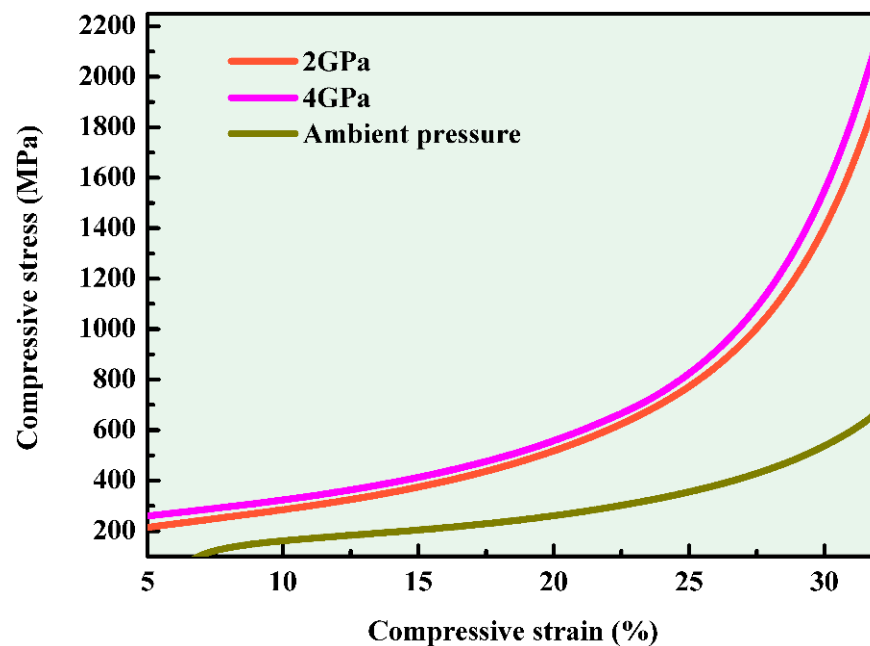


Figure 5. Compressive stress–strain curves of Al-5.4Ni-2Sn alloy at different pressures.

To make sure that the improvement of the strength of the alloy under high pressure is due to the solid solution strengthening effect of each phase, the hardness of α -Al phase and β -Sn phase after being solidified under different pressure conditions were detected and demonstrated in Table 3. The results show that the hardness values of α -Al phase increase progressively with the increase of pressure, while, for β -Sn phase, it shows the opposite trend. Compared with the ambient pressure, the hardness values of α -Al phase at ambient pressure, 2 GPa and 4 GPa are 1.5 GPa, 1.62 GPa and 1.99 GPa, respectively. The hardness values of α -Al phase increase by 8% and 32.7%, respectively, at high pressure. The hardness of β -Sn phase at ambient pressure, 2 GPa and 4 GPa is 1.09 GPa, 0.86 GPa and 0.75 GPa, respectively. The hardness of β -Sn phase decreases by about 31.2% at 4 GPa. The stress–strain curves of α -Al phase calculated from the nano-hardness results are shown in Figure 6b. The tensile strength of α -Al phase increases with the increase of solidification pressure.

Table 3. The nano-hardness of α -Al and β -Sn phase solidified at different pressures.

Phase	Ambient Pressure	2 GPa	4 GPa
α -Al	1.5	1.62	1.99
β -Sn	1.09	0.86	0.75

According to EDS and the above analysis, the content of Sn element in β -Sn phase increases gradually with the increase of pressure, while the hardness shows an opposite trend. The content of Ni element and Sn element in α -Al phase increases gradually with the increase of pressure. As a result, the hardness and strength of α -Al phase are greatly improved. In conclusion, the solid solution of Ni and Sn atoms in α -Al phase is conducive to the improvement of alloy strength, but the content of Sn should not be too much.

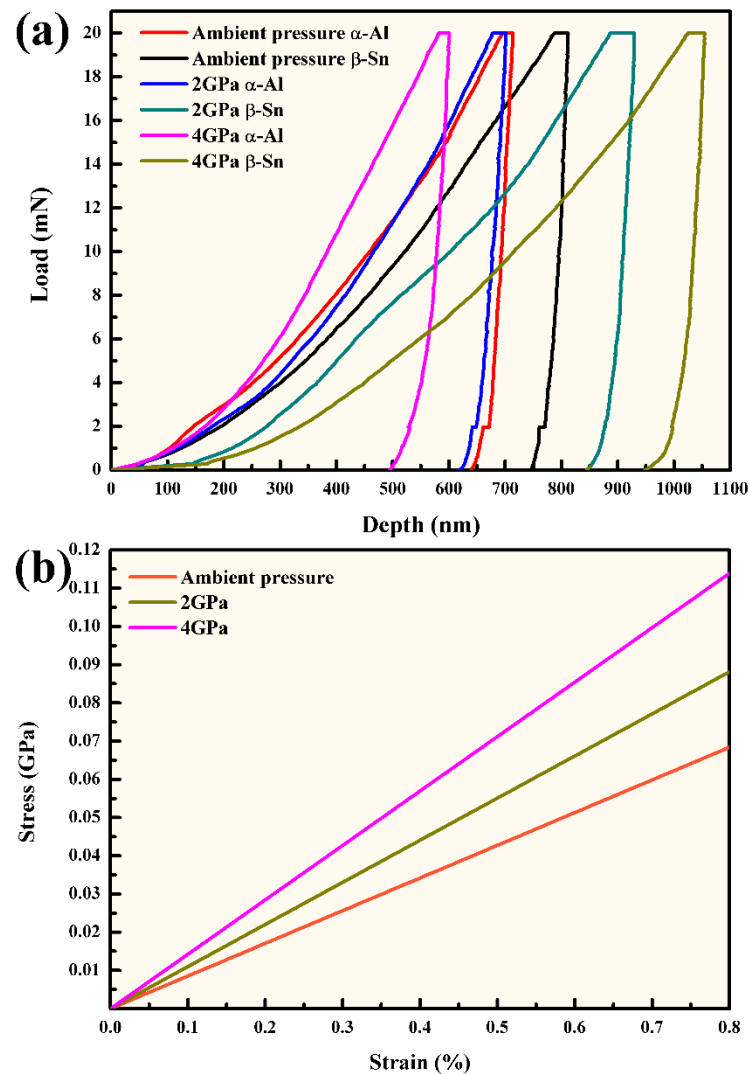


Figure 6. The nano-hardness measurement of α -Al phase and β -Sn phase. (a) The load–depth curve of α -Al phase and β -Sn phase, (b) the stress–strain curves of α -Al phase.

4. Conclusions

In this paper, the microstructure, phase composition and mechanical properties of Al-5.4Ni-2Sn alloy solidified under different pressures are researched. Meanwhile, the phase diagram of Al-5.4Ni-2Sn alloy solidified under equilibrium is calculated. The conclusions are shown as follows:

- (1) After solidification under different pressures, the Al-5.4Ni-2Sn alloy consists of α -Al phase, bulk Al_3Ni phase, interphase β -Sn and eutectic microstructure. Under high pressure, the thickness of β -Sn phase decreases obviously.
- (2) The precipitation sequence of the alloy during ambient pressure equilibrium solidification is $L \rightarrow \text{Al}_3\text{Ni} \rightarrow (\alpha\text{-Al} + \text{Al}_3\text{Ni})_{\text{eutectic}} \rightarrow (\alpha\text{-Al} + \text{Al}_3\text{Ni} + \beta\text{-Sn})_{\text{eutectic}}$.
- (3) The hardness values of α -Al phase at ambient pressure, 2 GPa and 4 GPa are 1.5 GPa, 1.62 GPa and 1.99 GPa, respectively. The tensile strength of the α -Al phase increases with the increase of solidification pressure.
- (4) The compressive strength and strain of the Al-5.4Ni-2Sn alloy under high pressure are obviously improved compared with those of the samples solidified under ambient pressure. When the deformation is 30%, the compressive strength at ambient pressure, 2 GPa and 4 GPa is 538.1 MPa, 1403.2 MPa and 1547.9 MPa respectively. The compressive strength under high pressure increased by 160.85% and 187.7%.

Author Contributions: Conceptualization, D.Z. and Y.C.; methodology, J.G., Z.Z. and X.Y.; software, F.L.; formal analysis, X.W., D.Z. and Y.C.; investigation, F.L. and Z.Z.; resources, X.Y.; data curation, X.Y. and F.L.; writing—original draft preparation, X.Y.; writing—review and editing, X.W., D.Z. and J.T.; supervision, D.Z.; project administration, D.Z.; funding acquisition, X.Y. All authors have read and agreed to the published version of the manuscript.

Funding: This work was supported by the National Natural Science Foundation of China [Nos. 52071165, 51771083].

Institutional Review Board Statement: Not applicable.

Informed Consent Statement: Not applicable.

Data Availability Statement: Not applicable.

Conflicts of Interest: The authors declare no conflict of interest.

References

1. Jambur, V.; Tangpatjaroen, C.; Xi, J.; Tarnsangpradit, J.; Gao, M.; Sheng, H.; Perepezko, J.H.; Szlufarska, I. Effects of minor alloying on the mechanical properties of Al based metallic glasses. *J. Alloys Compd.* **2021**, *854*, 157266. [[CrossRef](#)]
2. Das, S.; Mondal, D.P.; Sawla, S.; Ramakrishnan, N. Synergic effect of reinforcement and heat treatment on the two body abrasive wear of an Al–Si alloy under varying loads and abrasive sizes. *Wear* **2008**, *264*, 47–59. [[CrossRef](#)]
3. Liu, S.Q.; Wang, X.; Zu, Q.; Han, B.H.; Han, X.; Cui, C.X. Significantly improved particle strengthening of Al–Sc alloy by high Sc composition design and rapid solidification. *Mater. Sci. Eng. A* **2021**, *800*, 140304. [[CrossRef](#)]
4. Nie, Z.R. Function and development of alloy elements in aluminum. *Chin. J. Nonferr. Metal.* **2009**, *22*, 56–57.
5. Yun, K.; Li, S.R.; Li, W.X. Effects of transition metals, Fe, Ni, Sc and Zr, on the microstructure and mechanical properties of 2618 aluminum alloy. *Rare Met. Mater. Eng.* **2000**, *29*, 177–181.
6. Nandi, P.; Suwas, S.; Subodh, K. The Effect of minor addition of Ni on the microstructural evolution and mechanical properties of suction cast Al–0.14 at.pct Sc binary alloy. *Metall. Mater. Trans. A* **2013**, *44*, 2591–2603. [[CrossRef](#)]
7. Adachi, H.; Osamura, K.; Ochiai, S.; Jun, K.S.; Kazuhiko, Y. Mechanical property of nanoscale precipitate hardening aluminum alloys. *Scr. Mater.* **2001**, *44*, 1489–1492. [[CrossRef](#)]
8. Saadat, Z.; Moghanaki, S.K.; Kazeminezhad, M.; Goodarzi, M.; Afjeh, S.M.B.G. Effect of two steps annealing on the microstructure and dynamic strain aging behavior of Al–6Mg alloy. *Mater. Sci. Eng. A* **2020**, *798*, 140097. [[CrossRef](#)]
9. Compton, D.N.; Cornish, L.A.; Witcomb, M.J. The effect of microstructure on hardness measurements in the aluminium-rich corner of the Al–Ni–Cr system. *J. Alloys Compd.* **2001**, *317–318*, 372–378. [[CrossRef](#)]
10. Belov, N.A.; Zolotarevskiy, V.S. The Effect of Nickel on the Structure, Mechanical and Casting Properties of Aluminium Alloy of 7075 Type. *Mater. Sci. Forum* **2002**, *396–402*, 935–940. [[CrossRef](#)]
11. Zhao, Y.B.; Wang, Z.L.; Zhang, L.B. Effect of Ni on properties of ZL101A aluminum alloy. *Spec. Cast. Nonferr. Alloy* **2013**, *33*, 191.
12. Chen, D.H.; Chen, C.; Zhu, X.R. Squeeze casting and strengthening mechanism of high strength Al–Ni cast aluminum alloy. *Rare Met. Mater. Eng.* **2017**, *46*, 3525–3531.
13. Li, X.; Xie, H.; Zhang, Y.L.; Wei, X. Power Factor Optimization and Thermoelectric Properties of Mg₂Si_{1-x}Sn_x Alloys by Directional Solidification. *Rare Met. Mater. Eng.* **2020**, *49*, 2779–2785.
14. Xu, Z.; Utton, C.; Tsakiroopoulos, P.A. Study of the Effect of 5 at.% Sn on the Micro-Structure and Isothermal Oxidation at 800 and 1200 degrees C of Nb–24Ti–18Si Based Alloys with Al and/or Cr Additions. *Materials* **2020**, *13*, 245. [[CrossRef](#)]
15. Billur, C.A.; Saatçi, B. Experimental determination of interfacial energy for solid Al in the Al–Sn–Mg eutectic system with Bridgman-type apparatus. *Phys. Lett. A* **2019**, *383*, 2652–2657. [[CrossRef](#)]
16. Chen, X.; Zhang, D.F.; Xu, J.Y.; Feng, J.K.; Zhao, Y.; Jiang, B.; Pan, F.S. Improvement of mechanical properties of hot extruded and age treated Mg–Zn–Mn–Ca alloy through Sn addition. *J. Alloys Compd.* **2020**, *850*, 156711. [[CrossRef](#)]
17. He, C.Y.; Wang, J.G.; Chen, Y.L.; Yu, W.; Tang, D. Effects of Sn and Sb on the Hot Ductility of Nb plus Ti Micro-alloyed Steels. *Metals* **2020**, *10*, 1679. [[CrossRef](#)]
18. Ma, J.X.; Wei, Q.; Le, T.H.; Wang, J.H.; Jin, P.P. Effect of Sn addition on the microstructure and mechanical properties of AZ31 alloys. *Mater. Res. Express* **2020**, *7*, 126507. [[CrossRef](#)]
19. Ma, P.; Zou, C.M.; Wang, H.W.; Scudino, S.; Fu, B.G.; Wei, Z.J.; Kuhn, U.; Eckert, J. Effects of High Pressure and SiC Content on Microstructure and Precipitation Kinetics of Al–20Si alloy. *J. Alloys Compd.* **2014**, *586*, 639–644. [[CrossRef](#)]
20. Liu, X.; Ma, P.; Jia, Y.D.; Wei, Z.J.; Suo, C.J.; Ji, P.C.; Shi, X.R.; Yu, Z.S.; Prashanth, K.G. Solidification of Al–xCu alloy under high pressures. *J. Mater. Res. Technol.* **2020**, *9*, 2983–2991. [[CrossRef](#)]
21. Wang, H.W.; Zhu, D.D.; Zou, C.M.; Wei, Z.J. Evolution of the microstructure and nanohardness of Ti–48 at.%Al alloy solidified under high pressure. *Mater. Des.* **2012**, *38*, 1790–1796. [[CrossRef](#)]
22. Emuna, M.; Greenberg, Y.; Hevroni, R.; Korover, I.; Makov, G. Phase Diagrams of Binary Alloys under Pressure. *J. Alloys Compd.* **2016**, *687*, 360–369. [[CrossRef](#)]

23. Wang, S.M.; He, D.W.; Zou, Y.T.; Wei, J.J.; Lei, L.; Li, Y.J.; Wang, J.H.; Wang, W.D.; Kou, Z.L. High-pressure and high-temperature sintering of nanostructured bulk NiAl materials. *J. Mater. Res.* **2011**, *24*, 2089–2096. [[CrossRef](#)]
24. Jie, J.C.; Zou, C.M.; Brosh, E.; Wang, H.W.; Wei, Z.J.; Li, T.J. Microstructure and mechanical properties of an Al–Mg alloy solidified under high pressures. *J. Alloys Compd.* **2013**, *578*, 394–404. [[CrossRef](#)]
25. Fan, Z.; Lin, X.; Xu, R.; Dong, Y.; Wang, L.; Zhao, S.S. Electron back-scattering diffraction preliminary analysis of heterogeneous nuclei in magnesium alloy during solidification process under GPa high pressure. *J. Rare Earth* **2018**, *36*, 184–189. [[CrossRef](#)]
26. Fu, H.; Liu, N.; Zhang, Z.W.; Peng, Q.M. Effect of super-high pressure on microstructure and mechanical properties of Mg₉₇Zn₁Y₂ alloys. *J. Magnes. Alloy.* **2016**, *4*, 302–305. [[CrossRef](#)]
27. Dong, Y.; Lin, X.P.; Xu, R.; Zheng, R.G.; Fan, Z.B.; Liu, S.J.; Wang, Z. Microstructure and compression deformation behavior in the quasicrystal-reinforced Mg-8Zn-1Y alloy solidified under super-high pressure. *J. Rare Earth* **2014**, *32*, 1048–1055. [[CrossRef](#)]
28. Xu, S.; Xu, X.; Xu, Y.; Liang, Y.; Lin, J. Phase transformations and phase equilibria of a Ti-46.5Al-16.5Nb alloy. *Mater. Des.* **2016**, *101*, 88–94. [[CrossRef](#)]